3-D structure of the transition from convergent to transform margin in northern California as a proxy for San Andreas Fault System evolution

Principal investigators: Deborah Kilb (Scripps Institution of Oceanography, UCSD) and Vera Schulte-Pelkum (Cooperative Institute for Research in Environmental Sciences and Department of Geological Sciences, CU Boulder)

Abstract

We investigate the onshore transition from the transform plate boundary of the San Andreas Fault System (SAFS) to the convergent plate boundary of the Cascadia subduction zone in Northern California. Details of this transition zone, such as the geometry of the southern edge of the Cascadia slab and the presence and extent of a Pioneer detachment south of the slab edge, are still unknown and are of importance to seismic hazard in the region. Recently published new findings on low frequency earthquakes (LFEs) and tremor clusters south of the previously mapped Cascadia slab tremor band suggest modifications to the slab geometry and Pioneer detachment extent may be needed. We use shear fabric contrasts as imaged by receiver functions in conjunction with local relocated seismicity catalogs, the SCEC Community Fault Model (CFM), and recent catalogs of low-frequency earthquakes and tremor to investigate these features. We find a peak in the receiver function shear fabric signal at several stations atop the proposed Pioneer detachment that matches the depth of the proposed detachment ($\sim$20 km). Strikes of these arrivals are roughly N-S and similar to that of the motion of the proposed Pioneer fragment relative to the overriding North American Plate. These N-S strikes extend to the East into the region of newly located tremor. Near the transition to the subduction zone, strikes rotate to roughly E-W, similar to the strike of the band of LFEs and a previously imaged low velocity zone. Our findings support the presence of a Pioneer detachment.

Introduction The Mendocino Triple Junction region routinely hosts M5+ events (e.g., *Yeck et al.*, 2023) and connects the two largest plate boundary fault systems in the contiguous U.S., the Cascadia subduction zone and the SAFS. Recent work suggests the possibility of coordinated ruptures of the northern SAFS and Cascadia megathrust (*Goldfinger et al.*, 2025) across the transition zone. Capture of a Pioneer fragment by the Pacific plate was previously proposed based on tomographic images (*Furlong et al.*, 2024). A band of LFEs coincides in location and depth with the northern edge of the proposed Pioneer fragment (*Shelly et al.*, 2025) and shows focal mechanisms consistent with interaction of a Pioneer fragment with the slab edge (*Shelly et al.*, 2026). Recently found tremor clusters (*Lu and Ide*, 2026) extend south and west of the previously mapped tremor band on the Cascadia slab interface (*Wech*, 2021) and may be related to a Pioneer detachment or require modification of the southern slab edge geometry. The presence of a laterally extensive detachment fault is likely to affect seismic hazard in the region and may play a role in SAFS-Cascadia event interactions such as proposed by *Goldfinger et al.* (2025).

Methods and data Fault fabric contrasts were obtained from receiver functions for existing stations. We analyzed data from broadband three-component stations of the Northern California (NC), Berkeley (BK), Transportable Array (TA), and Plate Boundary Borehole Seismic (PB) networks for years 1998 to 2025. Receiver functions were calculated

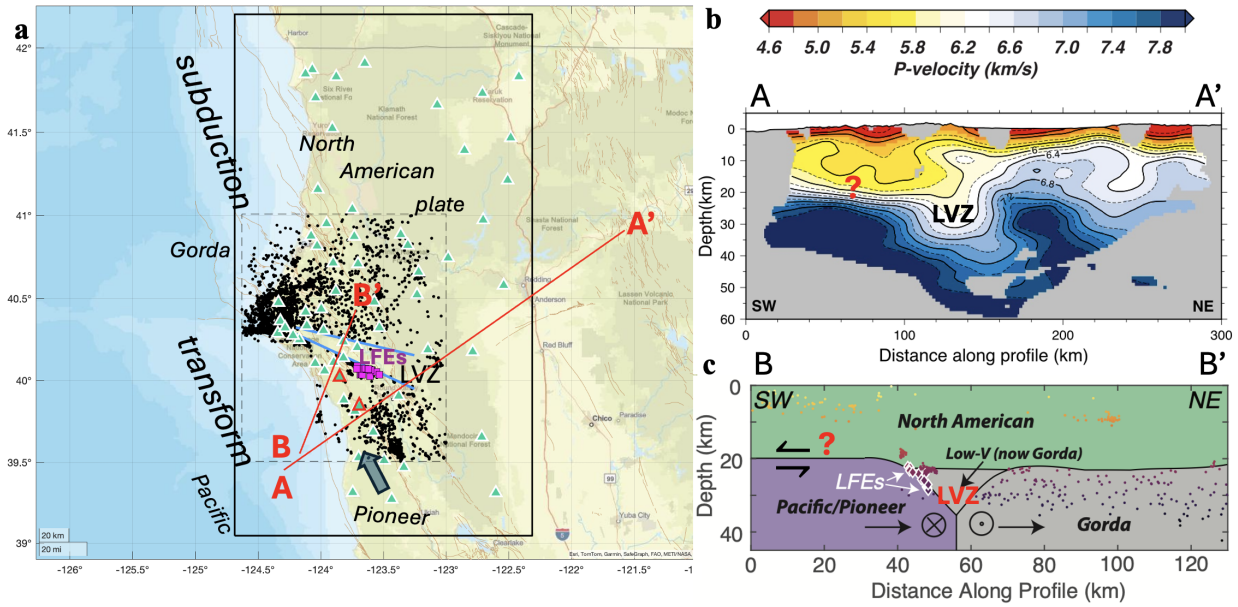

Figure 1: a) Map of subduction-transform transition area. Fault surface traces from USGS quaternary fault database in tan. Stations with receiver function results shown as blue triangles; two stations in Fig. 2 outlined in red. Seismicity relocated by *Shelly et al.* (2025) as black dots; the catalog covers the area outlined by the smaller box. Larger box indicates map area in Fig. 3. Low frequency earthquakes (LFEs) located by *Shelly et al.* (2025) as magenta squares. Blue lines bracket approximate extent of a low-velocity zone (LVZ) at ~20-35 km depth (*Furlong et al.*, 2024) that is accompanied by a lack of seismicity. Red lines show approximate locations of profiles in panels b and c. b) Depth section modified from tomographic image by *Furlong et al.* (2024). Red question mark shows possible Pioneer detachment with shear fabric that may be imaged by receiver functions. c) Interpretive sketch modified from *Shelly et al.* (2025). A Pioneer fragment is proposed to be captured and move with the Pacific plate. The LVZ is proposed to be North American material accreted to and now subducting with the Gorda slab. Red question marks indicate fabric contrasts interrogated with receiver functions.

and analyzed according to the process detailed in *Schulte-Pelkum and Mahan* (2014) and *Schulte-Pelkum et al.* (2020b). The method detects contrasts in Vp anisotropy and determines the depth of the contrast, the strike of foliation at the contrast, and the dip sense of foliation. In previous studies, this method was used to image regional fault fabric in southern California (*Schulte-Pelkum and Mahan*, 2014) and Alaska (*Schulte-Pelkum et al.*, 2020a), detachment faults in Alaska (*Schulte-Pelkum et al.*, 2025) and the Appalachians (*Frothingham et al.*, 2022), lithospheric shear zones (*Schulte-Pelkum and Kilb*, 2024), and volcanomagmatic fabrics (*Schulte-Pelkum and Haney*, 2024). Arrival times were migrated to depth with the same velocity model as that used for relocated seismicity and LFEs (*Shelly et al.*, 2025). Results were placed in spatial context with the Statewide California Data Center's Community Fault Model (SCEC CFM; *Plesch et al.* (2007)), relocated seismicity LFEs (*Shelly et al.*, 2025), and tremor (*Lu and Ide*, 2026).

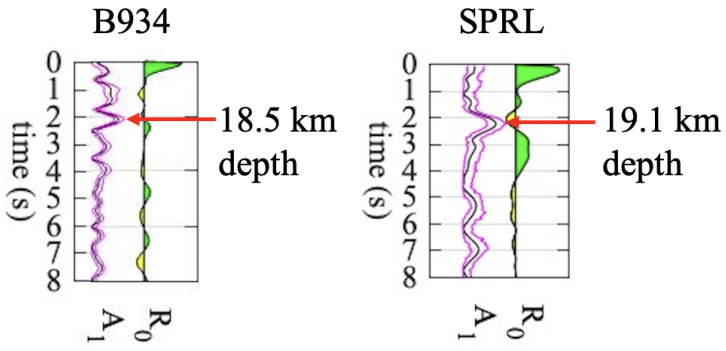

Figure 2: Receiver function examples from two stations marked with red outlines in Figure 1a; B934 is south of the LFE cluster, SPRL west of the LFEs. R_0 in green (positive amplitude) and yellow (negative amplitude) is the azimuthally averaged radial receiver function. A_1 (blue, bootstrap uncertainty range in magenta) is the first azimuthal harmonic solution; a peak in A_1 corresponds to an out-of-plane arrival in the radial and transverse component receiver functions with sin(azimuth)-periodic polarity flips from a contrast in plunging axis anisotropy. Amplitude scale for R_0 and A_1 is absolute and is the same for both stations. Red arrows mark possible arrival from anisotropic shear fabric on the Pioneer detachment at each station near 2o km depth, consisting of a high-amplitude A_1 peak at the expected depth and accompanied by a velocity reduction in the isotropic R_0 followed by a velocity increase below.

Results Previous studies have proposed the capture of an oceanic Pioneer fragment that subsequently began traveling northwestwards along with the Pacific plate (Figure 1a, c) on the outboard side of the San Andreas fault (e.g. *Furlong et al.*, 2024). A band of LFEs in the region (Figure 1a) were recently shown by *Shelly et al.* (2025) to be at the edge of a low-velocity zone (Figure 1b) previously imaged in tomographic studies (*Furlong et al.*, 2024). They were hypothesized to mark the southern extent of the Gorda slab. More recent work on focal mechanisms of this group of LFEs (*Shelly et al.*, 2026) suggests that they occur on a surface dipping to the NE that accommodates right-lateral motion, which matches the relative movement between the Pacific and Gorda plates. *Shelly et al.* (2026) interpreted this observation as supporting the model of Pioneer fragment capture by the Pacific plate, as well as the identification of the low-velocity wedge (Figure 1b,c) as an accretionary prism now subducting with the Gorda plate.

The hypothesized Pioneer detachment, shear between the LVZ and Pioneer/Pacific block, and shear between the LVZ and overriding North American plate may generate contrasts in Vp anisotropy that are detectable via receiver functions (Figure 1b,c). Results from two station atop the proposed detachment are shown in Fig. 2. Station SPRL, south of the LFE band, shows a single strong A_1 arrival just after 2 s delay time, corresponding to 19 km depth. Station B934 to the west shows the largest A_1 arrival at a similar depth. The conversion is from a contrast in Vp anisotropy with plunging axis; if it were from a dipping contrast with an isotropic Vs velocity jump, it would have to be accompanied by an equal amplitude peak at zero delay time (*Schulte-Pelkum and Mahan*, 2014), but

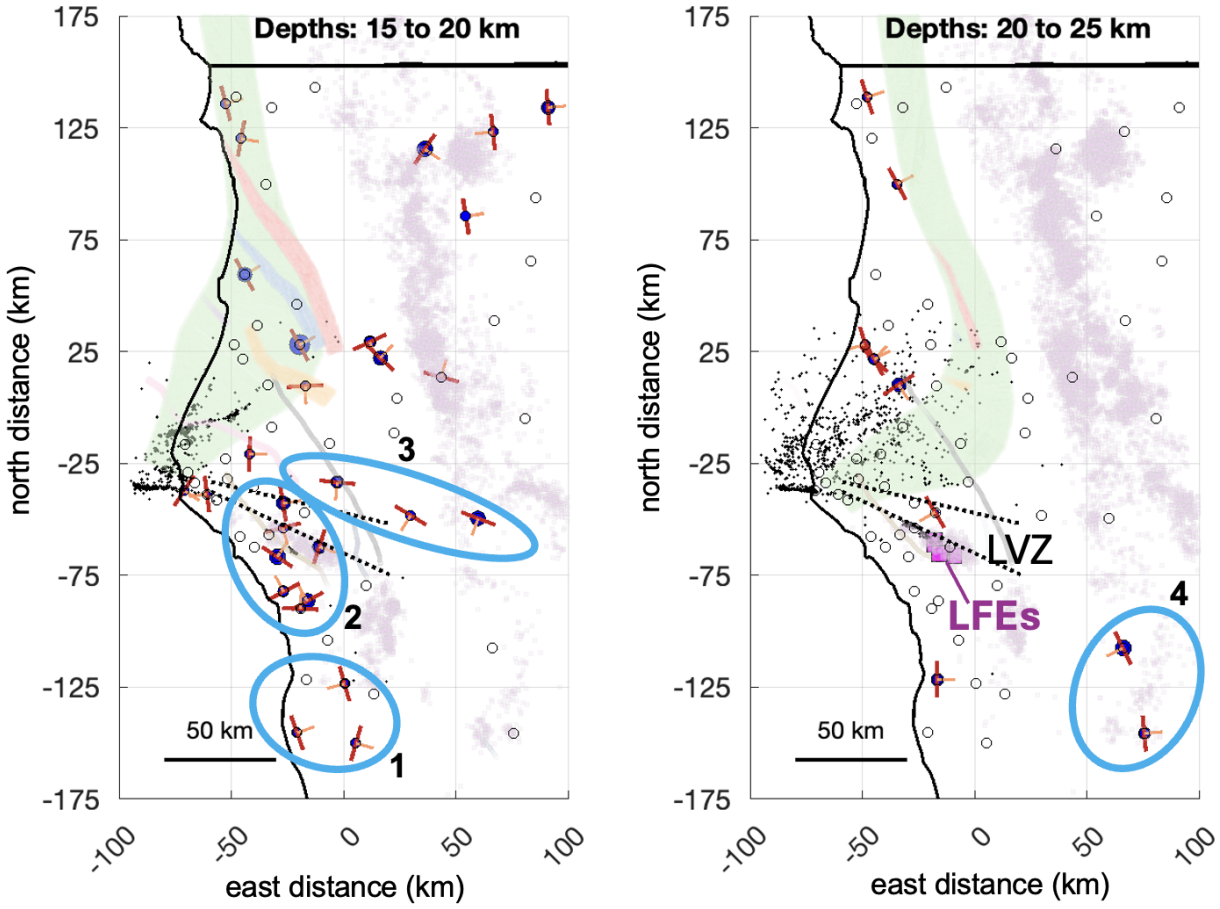

Figure 3: Depth slices in the larger inset box in Figure 1, showing the range of the proposed Pioneer detachment. SCEC CFM fault surfaces in semitransparent colors plotted in 3D view in each depth range (megathrust in green). Seismicity in each depth interval as black dots, and LVZ outlined in black dotted lines, LFEs as magenta squares, all from *Shelly et al.* (2025). Tremor from *Lu and Ide* (2026) in pink (semitransparent). Station locations with receiver function results shown as circles; empty where no A_1 arrival is seen from that depth range, blue fill where arrival is present. Circle size scales with amplitude of the A_1 arrival. Red bars show strike of fabric (strike of plane perpendicular to an anisotropic symmetry axis), orange tick marks are phase of A_1 and point downdip if anisotropy is stronger below the converter depth, updip if stronger above. Station groups outlined in cyan labeled with numbers refer to discussion in text.

amplitudes at zero delay are small for both stations. The arrivals are consistent with a Pioneer detachment near 20 km depth. Other stations in the area show peaks from this depth range as well (Figure 3). The large A_1 are accompanied by smaller amplitude R_0 arrivals with negative polarity, which imply a weakly low-velocity shear layer atop the detachment. They are followed by a deeper positive amplitude R_0 arrival implying an incerase in isotropic velocity entering the Pioneer fragment.

Receiver function results in context with the fault model, seismicity, and LFE positions are shown in Figure 3. Each panel shows a 5 km thick horizontal slice through the 3-dimensional model including SCEC CFM fault surfaces, relocated seismicity and LFEs from *Shelly et al.* (2025), and receiver function conversions from fabric contrasts within each depth range. Receiver functions were migrated to depth using the velocity model of *Yoon and Shelly* (2024), consistent with the relocations for seismicity and LFEs in *Shelly et al.* (2025), so depths can be compared directly. Tremor from *Lu and Ide* (2026) is also plotted in each depth range.

The Cascadia megathrust is shown in green in the depth slices. Slab dips and geometries in this region vary, with the USGS Slab2.0 model (*Hayes*, 2018) showing steeper dips and extending farther south (e.g. *McCrory et al.*, 2006). Other studies show shallower dips (*Bloch et al.*, 2023) more similar to the SCEC CFM. *Furlong et al.* (2024) proposes slab termination at the northern edge of the LVZ and seismicity gap, marked by dashed lines in Figure 3. The 15-20 km depth slice shows pervasive A_1 arrivals, particularly concentrated south of the LVZ in the region of the proposed Pioneer detachment (groups labeled 1 and 2 in Figure 3). Strikes are approximately N-S in the southernmost group 1, similar to the shear sense of the Pioneer fragment relative to the overlying North American plate. Strikes rotate to more E-W orientations in group 2 approaching the LFE cluster and the LVZ at 5 stations. *Shelly et al.* (2026) suggest two types of shear at the southern edge of the LVZ (Fig. 1c), bottom-to-the-north shear at the Pioneer detachment and right-lateral strike-slip motion between the Pioneer fragment and the Gorda plate, which may cause the chance in strikes. Two stations in group 2 within the LVZ show N-S strikes.

Moving north of the LVZ, stations in group 3 show strikes paralleling the LVZ. The deeper section from 20 to 25 km shows fewer A_1 (Figure 3). Group 4 shows two stations atop the tremor cluster III from *Lu and Ide* (2026) with approximately N-S strikes, similar to group 1 in the shallower depth slice. Explaining this cluster as occurring on an interface would require either extending the slab farther south if the cluster is interpreted as a continuation of the Cascadia tremor band or an extension of the Pioneer fragment to the east if the tremor and A_1 arrivals are interpreted as stemming from the Pioneer detachment. Either option would be permissible by the A_1 orientations.

Conclusions Receiver function analysis supports the presence of a Pioneer detachment. More detailed interpretation of recent tremor locations, LFE results, and imaging is warranted, and the results from this project form the basis of a proposed Technical Activity Group.

References Cited

Bloch, W., M. G. Bostock, and P. Audet, A Cascadia Slab Model From Receiver Functions, *Geochemistry, Geophysics, Geosystems*, *24*(10), e2023GC011088, doi:10.1029/2023GC01108810.31223/x59t0g, 2023.

Frothingham, M. G., V. Schulte-Pelkum, K. H. Mahan, A. J. Merschat, M. Mather, and Z. C. Gomez, Don't judge an orogen by its cover: Kinematics of the Appalachian décollement from seismic anisotropy, *Geology*, *50*, 1306–1311, doi:10.1130/G50323.1, 2022.

Furlong, K. P., A. Villaseñor, H. M. Benz, and K. A. McKenzie, Formation and Evolution of the Pacific-North American (San Andreas) Plate Boundary: Constraints From the Crustal Architecture of Northern California, *Tectonics*, *43*(6), e2023TC007963, doi:10.1029/2023TC007963, 2024.

Goldfinger, C., J. Beeson, B. Black, A. Vizcaino, C. H. Nelson, A. Morey, J. R. Patton, J. Gutiérrez-Pastor, C. Romsos, and M. D. Walzcak, Unravelling the dance of earthquakes: Evidence of partial synchronization of the northern San Andreas fault and Cascadia megathrust, *Geosphere*, *21*(6), 1132–1180, doi:10.1130/GES02857.1, 2025.

Hayes, G., A Comprehensive Subduction Zone Geometry Model U.S. Geological Survey data release, *U.S. Geological Survey data release*, doi:10.5066/F7PV6JNV, 2018.

Lu, W., and S. Ide, Spatiotemporal Characteristics of Tectonic Tremors in California, , *53*(4), e2025GL120742, doi:10.1029/2025GL120742, 2026.

McCrory, P., J. Blair, D. Oppenheimer, and S. Walter, Depth to the Juan De Fuca slab beneath the Cascadia subduction margin – A 3-D model for sorting earthquakes, *U.S. Geological Survey Data Ser. 91*, 2006.

Plesch, A., J. H. Shaw, C. Benson, W. A. Bryant, S. Carena, M. Cooke, J. Dolan, G. Fuis, E. Gath, L. Grant, E. Hauksson, T. Jordan, M. Kamerling, M. Legg, S. Lindvall, H. Magistrale, C. Nicholson, N. Niemi, M. Oskin, S. Perry, G. Planansky, T. Rockwell, P. Shearer, C. Sorlien, M. P. Suss, J. Suppe, J. Treiman, and R. Yeats, Community Fault Model (CFM) for Southern California, *Bulletin of the Seismological Society of America*, *97*(6), 1793–1802, doi:10.1785/0120050211, 2007.

Schulte-Pelkum, V., and D. Kilb, Lithospheric foundering in progress imaged under an extinct continental arc, *Geophysical Research Letters*, *51*(24), e2024GL111,290, doi:10.1029/2024GL111290, 2024.

Schulte-Pelkum, V., and K. H. Mahan, A method for mapping crustal deformation and anisotropy with receiver functions and first results from USArray, *Earth Planet. Sci. Lett.*, *402*, 221–233, 2014.

Schulte-Pelkum, V., and K. H. Mahan, A method for mapping crustal deformation and anisotropy with receiver functions and first results from USArray, *Earth Planet. Sci. Lett.*, *402*(SI), 221–233, doi:10.1016/j.epsl.2014.01.050, 2014.

Schulte-Pelkum, V., J. S. Caine, J. V. J. III, and T. W. B. Becker, Imaging the tectonic grain of the Northern Cordillera orogen using Transportable Array receiver functions, (in press), 2020a.

Schulte-Pelkum, V., A. M. Bender, and N. A. Ruppert, *Seismicity and Anisotropic Imaging Reveal an Active Detachment Beneath the Northern Alaska Range Foothills*, chap. 21, pp. 575–587, American Geophysical Union (AGU), doi:https://doi.org/10.1002/9781394195947.ch21, 2025.

Schulte-Pelkum, V. Z. R., K. Mueller, and Y. Ben-Zion, Tectonic inheritance with dipping faults and deformation fabric in the brittle and ductile southern California crust, *J. Geophys. Res.*, *125*(8), e2020JB019,525, doi:10.1029/2020JB019525, 2020b.

Schulte-Pelkum, V., and M. M. Haney, Fault–Dike–Magma Interactions Inferred from Transcrustal Conical Structures under Akutan Volcano, *Seismological Research Letters*, *95*(5), 2663–2673, doi:10.1785/0220240119, 2024.

Shelly, D. R., D. E. Goldberg, A. G. Wech, and A. M. Thomas, A northeast-dipping zone of low-frequency earthquakes at the southern edge of Cascadia subduction, , *52*(12), e2025GL116116, doi:10.1029/2025GL116116, 2025.

Shelly, D. R., A. M. Thomas, K. Materna, and R. J. Skoumal, Low-frequency earthquakes track the evolution of a captured slab fragment at the Mendocino Triple Junction, *SCEC Annual Meeting*, 2025.

Shelly, D. R., A. M. Thomas, K. Z. Materna, and R. J. Skoumal, Low-frequency earthquakes track the motion of a captured slab fragment, *Science*, *391*(6782), 294–299, doi:10.1126/science.aeb2407, 2026.

Wech, A. G., Cataloging tectonic tremor energy radiation in the Cascadia subduction zone, *Journal of Geophysical Research: Solid Earth*, *126*(10), e2021JB022,523, doi:10.1029/2021JB022523, 2021.

Yeck, W. L., D. R. Shelly, K. Z. Materna, D. E. Goldberg, and P. S. Earle, Dense geophysical observations reveal a triggered, concurrent multi-fault rupture at the Mendocino Triple Junction, *Communications Earth and Environment*, *4*, doi:10.1038/s43247-023-00752-2, 2023.

Yoon, C., and D. Shelly, Distinct yet adjacent earthquake sequences near the Mendocino Triple Junction: 20 December 2021 Mw 6.1 and 6.0 Petrolia, and 20 December 2022 Mw 6.4 Ferndale, *The Seismic Record*, *2074*, 81–92, doi:10.1785/0320230053, 2024.